A study on the mechanical behaviour of WC/Co hardmetals

J.A.M. Ferreira *, M.A. Pina Amaral, F.V. Antunes, J.D.M. Costa

CEMUC, Department of Mechanical Engineering, University of Coimbra, Pinhal de Marrocos, 3030-788 Coimbra, Portugal

Abstract

The hardmetal cutting tools used in machining are submitted to extreme conditions in terms of temperature and mechanical loading. A better understanding of the failure of cutting tools and capability to predict tool life are key factors in the development of new tool materials with improved mechanical behaviour. Main failure mechanisms are wear, thermal–mechanical fatigue and brittle fracture. The aim of present work is to study the mechanical behaviour of two hardmetals. The properties studied were Young's modulus, bending strength, fracture toughness and fatigue endurance. The resonant technique was used to determine elastic properties and a good agreement was found with three-point bending results.
© 2008 Elsevier Ltd. All rights reserved.

Keywords: Hardmetal; Young's modulus; Fracture toughness; Fatigue behaviour

1. Introduction

Machining is an important operation in the production of industrial products, which must fulfill not only the dimensional and geometrical requirements, but also the surface integrity. Applied to almost all materials, this operation is used in many industrial sectors, and represents an important part of the cost of the final product. Tool replacement and machine adjusting involve time, decreasing productivity. Cost reduction is a great concern for the industrial competitiveness; therefore improvements in tool life are welcome.

Three complementary investigation lines can be identified for a feasible life prediction: a first one to determine mechanical and thermal loadings applied to the tool, a numerical approach to obtain stress and thermal fields, a third one that studies material behaviour under service conditions.

The mechanical and thermal loadings on the cutting tools depend on several parameters, namely, tool geometry and material (bulk material and coating), cutting parameters (cutting speed, advance, etc.), lubrication and material being machined. The three orthogonal components of the cutting force can be determined with dynamometers, while temperature analysis can be performed using an infrared equipment. In the recent decades, the finite element method (FEM) has become a powerful tool in the simulation of cutting processes [1,2].

The finite element method is also adequate to model the mechanical behaviour and identify tool critical points in terms of stress and temperature. Modelling requires the precise knowledge of geometry, loading, boundary conditions and material properties.

The development and optimisation of hardmetal cutting tools requires a deep knowledge of mechanical behaviour under service conditions. In cutting tools hardmetals are submitted not only to wear at elevated temperature, but also to static and cyclic thermo-mechanical loads. Therefore, there are several tool failure modes, namely catastrophic chipping and plastic deformation of the cutting edge, fatigue, and tool wear mechanisms like flank wear and crater wear [3]. Cyclic loads result from thermal cycling caused by repeated heating/cooling cycles of the cutting edge. The interrupted nature of the milling process

* Corresponding author. Tel.: +351 239790700; fax: +351 239790701.
  E-mail address: martins.ferreira@dem.uc.pt (J.A.M. Ferreira).

causes a high number of thermal cycles, but it also occurs in turning applications which use coolant. Additional cyclic loads result from vibration of machines, alternating slip and stick of chips and from interrupted cutting. Therefore knowledge about the behaviour of these materials under cyclic loads is also required. However, considering the brittle behaviour of these materials, fatigue initiation from inherent defects is predominant over propagation and S–N results are more adequate. Besides, near the cutting edge, the cutting materials are at elevated temperatures. Hence materials must be studied at elevated temperature to assess the behaviour under service conditions. Nonetheless, it has to be noted that larger parts of the cutting tools are at lower temperatures and experience the highest bending stress in the loaded tool. Most of the research has been concerned with mechanisms and processes that occur mainly at room temperature and in neutral environment.

The aim of this work is to study the mechanical behaviour of two WC/Co hardmetals at room temperature and at elevated temperature. Properties such as bending strength, fracture toughness and fatigue strength were determined. Fractures surfaces were studied by SEM to identify failure mechanisms. The elastic properties were also obtained using resonant technique.

2. Materials

Two hardmetals composed of WC/Co were studied. The average particle size, nominal Co percentage and hardness are indicated in Table 1. Fig. 1 shows the structure of material 2 observed by SEM.

Material 1 has a hardness of 1886 HV30, while material 2 has a hardness of 874 HV30. These results are nearly the

Table 1
Hardmetal characterization

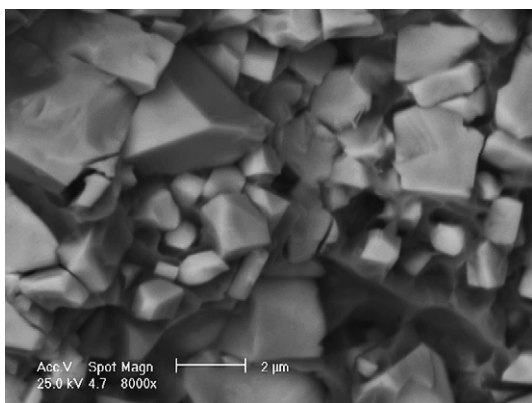| Material	Hardness HV30	Grain size (μm)	Nominal cobalt content (wt%)
1	1886	0.5	5
2	874	1.0	15

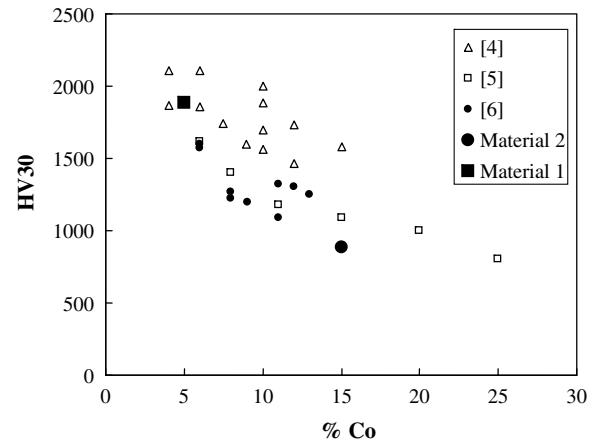
Fig. 1. Microstructure of material 2 observed by SEM.

Fig. 2. Hardness Vickers against Co weight fraction at room temperature.

lower band of literature results [4–6], as is shown in Fig. 2. The increase of cobalt reduces the hardness as could be expected, since this it is the soft phase. The scatter in Fig. 2 is explained by microstructural parameters other than Co percentage. Main microstructural parameters are Co percentage and particle size, which determine WC contiguity and Co average free path, but other parameters are shape and size distribution of carbides, porosity, impurities, etc.

3. Presentation and analysis of results

3.1. Young's modulus (E)

The elastic and thermal properties are fundamental for the numerical determination of stress and strain fields within cutting tools. Several experimental techniques have been used to determine elastic constants, which can be classified into static and dynamics techniques. Static methods determine elastic constants from the linear regions of stress-strain curves and include tensile tests, bending tests [7] and nanoindentation [8]. Dynamic methods include resonance and pulse techniques. Nanoindentation is adequate to obtain local values of rigidity, being widely applied to the analysis of thin films. Therefore is not adequate for heterogeneous materials, like hardmetals or laminated composites. Tension tests are also not adequate, considering the high rigidity and the brittle nature of the materials under study. The resonant beam technique is widely used to determine simultaneously both Young's modulus and the shear modulus of isotropic [9], orthotropic [10] and transversely isotropic [11] materials from the resonance frequencies of flexural vibrations. The elastic properties obtained are average values, suitable as input values for Finite Element Method analysis. The largest the specimen, the more representative will be the properties. It is a non destructive technique, known for their high reproducibility and accuracy [12]. Besides, the dynamic elastic behaviour characterized by modulus and damping, is important since it controls the vibrational response of structures. Therefore

the resonant technique was applied for the determination of Young's modulus (E).

The first natural frequency was determined experimentally on specimens with bar shapes $60 \times 10 \times 3$ mm. The technique is very sensitive to variations in dimensions, therefore well prepared samples with parallel and smooth surfaces are required. The specimen was suspended horizontally without significant constraint in order to simulate free–free boundary conditions during vibration. Other boundary conditions can be found in the literature [9], however free–free vibration is more adequate for experimental and numerical reproduction. A 2 mm strain gauge with minimum weight was glued on the specimen at half section, therefore does not influence natural vibration of the specimen. The signal was acquired using A/D acquisition data system. A singular elastic strike was applied with an impact tool for mechanical exciting and an electric signal proportional to local extension was acquired. Fig. 3a presents a typical signal of potential drop versus time for material 1. This signal shows no evidence of damping, which could be expected. FFT analysis transformed this signal into amplitude versus frequency, as illustrated in Fig. 3b. Further details can be found elsewhere [13]. The experimental frequencies are used to determine mechanical

properties considering analytical or numerical procedures. Analytical formulas have been developed to calculate elastic modulus (E) from the resonant frequencies of a beam shaped test sample. European and American standard test procedures, ENV-843-2 and ASTM C1259-96, respectively, propose the following equation to calculate Young's modulus along the main axis of beam like samples from the first flexural frequency (Fig. 4a)

$$E = 0.946 \frac{m \times f^2}{W} \left(\frac{L}{t} \right)^3 \times A_f \tag{1}$$

f being the resonant frequency, L the length, W the width, t the thickness and A_f a shape factor [11]. For other resonant modes (Fig. 4b) numerical methods may be used o determine relations between elastic properties and resonant frequencies.

A numerical analysis was developed to relate elastic properties with bending resonant frequencies. 3D isoparametric quadratic elements were used along with full integration. The material was assumed to be continuous, homogeneous, isotropic and with linear elastic behaviour. Soft springs were used to simulate constraints of experimental setup. Fig. 5 presents the final results of Young's
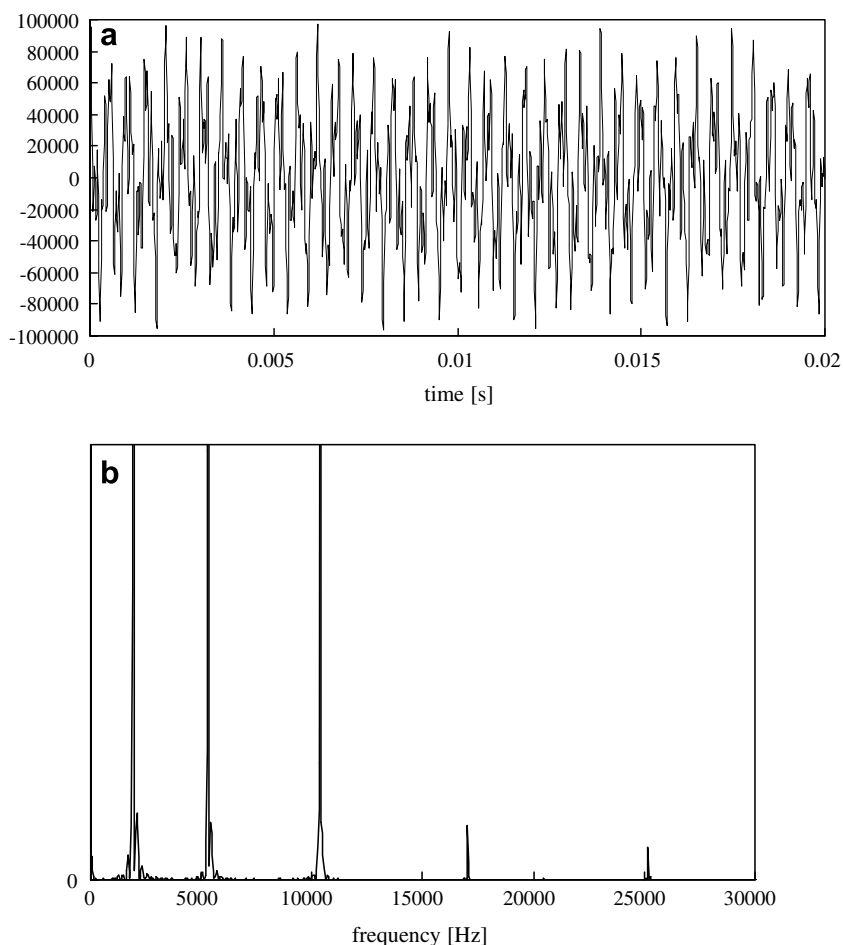

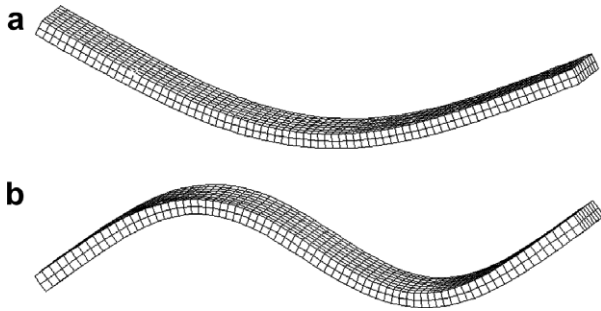Fig. 3. PD versus time plot and response in frequency domain.

Fig. 4. First bending resonant modes.

$$E_{hm} = (E_p V_p + E_{Co} V_{Co}) \quad\quad (2)$$

$$E_{hm} = \frac{E_p E_{Co}}{E_p V_{Co} + E_{Co} V_p} \quad\quad (3)$$

where V, E, p, Co and hm represent volume fraction, Young's modulus, particle, cobalt and hardmetal, respectively. Hirsch [15] proposed an intermediate model:

$$E_{hm} = x \cdot (E_p V_p + E_{Co} V_{Co}) + (1-x) \cdot \frac{E_p E_{Co}}{E_p V_{Co} + E_{Co} V_p} \quad (4)$$

For $x = 0$ and $x = 1$, Hirsch's equation reduces to Reuss and Voigt models, respectively. Parameter x is determined empirically. A third phase, the porosity, may be added to these models. Fig. 6 presents the predictions obtained for the composite for different x assuming $E_{Co} = 207$ GPa, $E_{WC} = 703$ GPa, $\rho_{Co} = 8800$ kg/m^3, $\rho_{WC} = 15700$ kg/m^3 [16]. The present results approach to Reuss equation. The curves that better fit the experimental points are using $x = 0$–0.25. However in literature are reported higher x values. For example, the results of Ingelstrom and Nordberg [5] cemented tungsten carbides are well fitted for $x = 0.5$–0.75.

modulus obtained for material 1 (assuming a Poisson's ratio $v = 0.27$). A slight decrease of E with resonant frequency can be observed.

Three-point bending tests within linear elastic regime were done to obtain material's rigidity using the same specimen dimensions of resonant tests in order to eliminate scatter associated with geometry. An average value $E = 596.7$ GPa was obtained for material 1, which is 5% below resonant technique value. Bending is the deformation mode in both resonant technique and tree-point bending technique. The differences can be explained by strain level (which is lower in resonant technique). In fact, the specimen is submitted to minute strains, hence the modulus are measured near the origin of the stress-strain curve. Deformation rate is not expected to explain the differences, considering the trend of Fig. 5 for different resonant frequencies.

For material 2 it was obtained $E = 418$ GPa, using resonant technique, also assuming $v = 0.27$. As expected, the increase of cobalt content reduces the rigidity of the hardmetal. Some damping was observed, which is also associated with cobalt increase.

Analytical models were used to model the elastic behaviour of hardmetals. Simplest and extreme approaches are Voigt and Reuss models, which assume parallel and serial arrangements, respectively [14]. The mathematical expressions of Voigt and Reuss models are respectively,
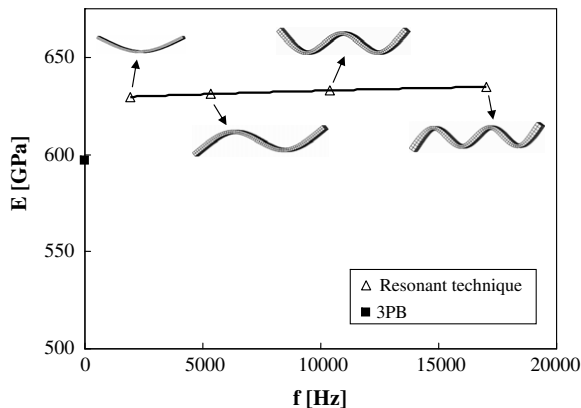
3.2. Mechanical strength

For mechanical strength and fatigue studies at room and elevated temperature a small specimen 5 mm thick and with reduced middle section was developed for three-point bending (Fig. 7). The midsection is a 5×5 mm square and is the location expected for fatigue and fracture failure. The geometry proposed is based on previous specimens geometries defined by Torres et al. [17] and Kindermann et al. [18]. The main aspects considered to define this geometry were the difficulty of manufacturing, volume of material, mechanical resistance and resolution of load measurement [19]. The geometry is relatively simple which simplifies production procedure. The size is expected to be within a reasonable range. Small size specimens are recommended to
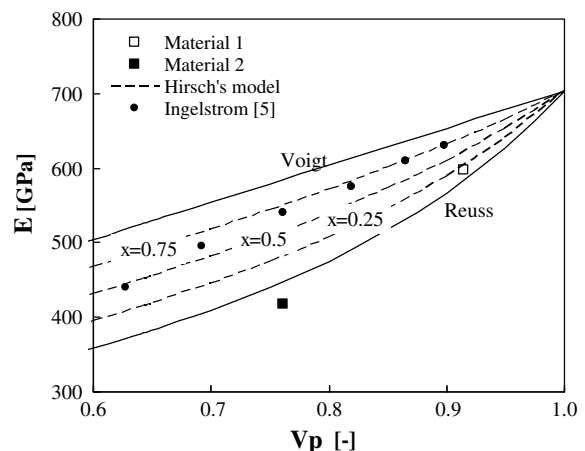

Fig. 5. Young's modulus versus resonant frequency for material 1.

Fig. 6. Experimental results and analytical models.
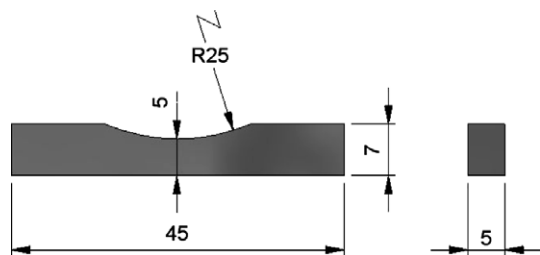
Fig. 7. Specimen geometry.

Fig. 8. Stress–strain curves for material 2.

reduce cost and to avoid exaggeratedly high loads. Besides, the furnace for elevated temperature testing imposes an upper limit for the size.

An electromechanical testing machine equipped with a furnace with temperature accuracy control better than 1 °C and adequate fixtures were used. For material 1 five specimens were tested at room temperature and three at 500 °C, respectively. The stress versus strain curves obtained for this material 1 were closed and nearly linear until final fracture typical of brittle. A slight tendency to decrease of the stiffness for the tests performed at 500 °C was observed. The slope of linear regions was used to measure Young's modulus but the values obtained by this technique are lower than the obtained by resonant technique which indicates that the global rigidity is not only being controlled by the specimen but also by the different components of three point bending apparatus which can be seen as serial springs, therefore Young's modulus must be obtained by an alternative approach. Anyway, the force applied on the specimen is not affected and bending strength (σ_{UTS}) can be measured from ultimate load. The results presented in Table 2 shows a great scatter at room temperature which indicates a great sensitivity to defects. In fact, the material presents very limited plastic deformation, which enables stress relaxation. The volume of material submitted to the highest stress is limited to the surface layer. Therefore, the presence of defects within this region is expected to affect the tensile strength. The sudden stress variation along the height indicates that subsurface defects are expected to have a limited influence. The increase of temperature seems to reduce tensile strength and the scatter. Scatter reduction could be expected since plastic deformation of cobalt increases which makes the material less sensitive to the presence of defects. For material 2 only two tests at each tem-
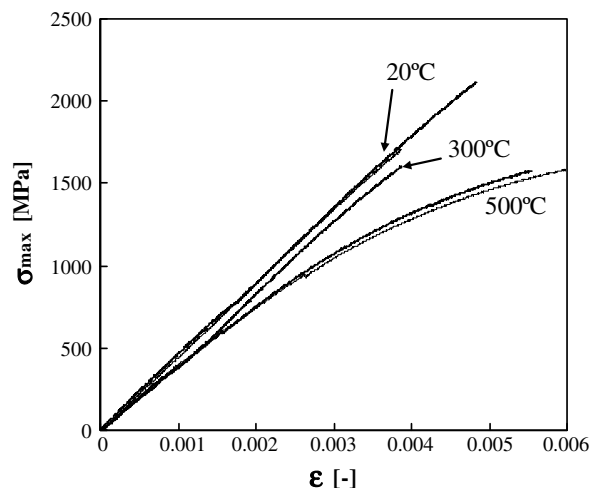
perature were performed at: room temperature, 300 °C and 500 °C. Fig. 8 presents some of the stress–strain curves obtained for material 2. Table 2 presents the global results obtained for the two materials. At room temperature and at 300 °C the material 2 exhibits a linear behaviour up to fracture, therefore with limited plastic deformation, which is according the brittle behaviour of this class of materials. However at 500 °C some plastic deformation can be observed, which is explained by a change in cobalt behaviour. This behaviour was not observed for material 1, since this has relatively low cobalt content. The increase of cobalt percentage increases tensile strength, as could be expected. The increase of temperature reduces σ_{UTS}, which is explained by modifications in Co behaviour.

3.3. Fracture toughness

The failure of these materials normally initiates at preexisting defects. Fracture toughness is a main property for the design of hardmetal cutting tools due to the high risk of brittle fracture. Besides, because the mechanisms of wear exhibited by cemented carbides are mainly mechanisms of surface fracture, the severity of wear must be largely controlled by the fracture toughness of the surface layers [6].

A classical test is the indentation technique proposed by Palmqvist in 1962. In this a Vickers indentation is done on material's surface and the length of cracks produced at the four corners (Palmqvist cracks) is measured. It requires only small samples along with standard equipment for hardness Vickers measurement, and specimen preparation consists of providing a polished, reflective plane surface. However, a major drawback is the sensitivity to surface stress state. Polishing and annealing are used to overcome this problem. Several equations are proposed in literature, assuming different ideal crack shapes [20]. Techniques based on pre-cracked specimens are also available, namely single edge notched beam, or single edge V-notched beam [17]. However, the brittle behaviour of the material, make

Table 2
Ultimate bending strength

Material	Temperature (°C)	σ_{UTS} (MPa)	Average (MPa)	SD/Aver (%)
1	20	1654; 1443; 1563; 1650; 1306	1523	9.7
	500	1517; 1422; 1458	1466	3.3
2	20	2114; 1710	1912	14.9
	300	2022; 1604	1813	16.3
	500	1584; 1577	1581	0.3

fatigue pre-cracking quite difficult since failure occurred immediately after crack initiation. Compressive loads and razor blades were used to obtain sharp pre-cracks. Ingelstrom and Nordberg [5] applied a compressive stress below the machined notch of CT specimens and impacted them with a wedge. The crack initiated arrested within compressive zone. The application of tension loads for pre-cracks usually produces premature failure. Often there is a discrepancy between Palmqvist indentation technique and conventional methods [17].

Fracture toughness of material 1 was studied with Palmqvist technique. Material's surface was polished and a load of 30 kgf was applied. Fracture toughness is given by

$$K_{lc} = 0.0889 \sqrt{\frac{HV \times F}{L_i}} \qquad (5)$$

where $L_i = a_1 + a_2 + a_3 + a_4$ the sum of corner cracks length, F the indentation load in Newton and HV the hardness Vickers in N/m^2

$$HV = 1.8544 \frac{P}{d^2} \qquad (6)$$

where d is average of the two diagonals of the indentation [m]. Fig. 9 presents the results obtained and a typical indentation. An average value of 9.3 MPa m$^{1/2}$ was obtained with a variation coefficient (standard deviation/average) of 3.2%.

Palmqvist toughness testing was also applied to material 2 but no cracks appeared at the corners of indentations, due to the relatively high cobalt content. Therefore fracture toughness was determined in notched three-point bending specimens without pre-cracking. A relation between fracture toughness of notched and cracked specimens ($K_{c,n}$) and K_{IC}, respectively, was considered, based on cleavage rupture criteria [21]:

$$\frac{K_{c,n}}{K_{IC}} = \frac{(1 + \rho/4r_0)^{3/2}}{1 + \rho/2r_0} \qquad (7)$$

ρ being the diameter of the notch and r_0 a short distance from crack tip [22]. Fig. 10 shows that the results obtained with this alternative technique are within literature results
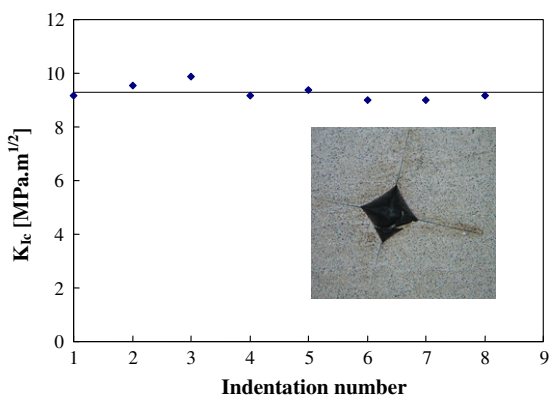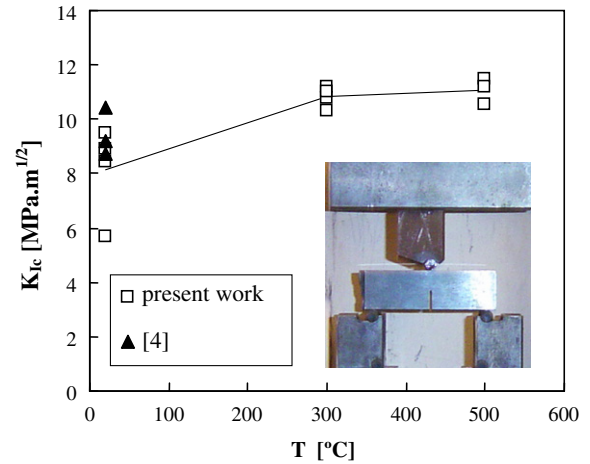

Fig. 10. Fracture toughness versus temperature for material 2.

and that the increase of temperature increases slightly the fracture toughness, as could be expected.

3.4. Fatigue

Two main approaches have been followed for fatigue studies. Llanes et al. [16] and Torres et al. [23] studied the fatigue crack propagation in these materials, namely the influence of K_{max}, ΔK, load ratio and microstructural parameters on fatigue crack growth rate (da/dN). On the other hand Schleinkofer et al. [24,25] and Roebuck et al. [26] obtained S–N curves. According to Schleinkofer fatigue strength of these materials is quite low than static strength and the failure of crack tip is complex and controlled predominantly by the ductile phase of the material.

Preliminary results showed that fatigue initiation from inherent defects is predominant over propagation; therefore S–N results are more adequate. A fatigue study was developed using a servo-hydraulic machine, three-point bending specimens with the geometry indicated in Fig. 7 and a furnace. The parameters studied were maximum stress, stress ratio ($R = 0.05$ and $R = 0.5$) and temperature

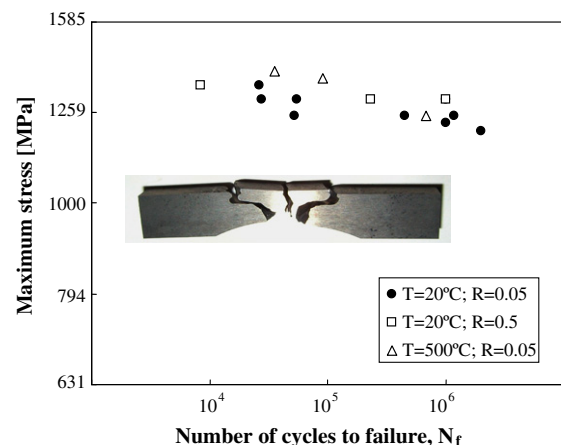Fig. 9. Fracture toughness of material 1 for various indentations.

Fig. 11. S–N fatigue results for material 1.

(20 °C and 500 °C). Fig. 11 presents the results obtained for material 1 and a typical fractured specimen. The behaviour was found to be dependent mainly on maximum stress, which indicates that failure is associated with static mechanisms. A great scatter can be observed, which is in agreement with static strength results.

The fracture initiation sites are usually processing heterogeneities whose sizes are proportional to the carbide mean size. Critical fracture crack size is very little. For example assuming $K_{max} = 8$ MPa $\sqrt{m}$ and a maximum stress of 1300 MPa the critical flaw size will be about 0.028 mm, a macrostructural value but only few times the material grain size. For these materials fatigue crack propagation regime will be very short. Short defects localized in regions highly stressed conduce to an easy crack initiation which is strong dependent of the material heterogeneities.

The fatigue live seems to be mainly influenced by maximum stress instead of the alternate stress with negligible influence of the stress ratio. By other side the results of these tests show that the material exhibits slightly higher fatigue strength at 500 °C than at room temperature. This is in agreement with the Roebuck et al. [26] conclusions and is explained by the changes in the residual stresses between the carbide and the binder phases and its relationship with microcrack initiation.

4. Conclusions

The Young's modulus, bending strength, fracture toughness and fatigue endurance were obtained for two hardmetals. The resonant technique was used to determine elastic properties as alternative to traditional three-point bending tests conducting to most accurate and feasible results.

Flexural tests are more adequate than tensile tests for studying mechanical strength in WC–Co alloys. The material 1 exhibits a brittle behaviour at room temperature and 300 °C and some plastic deformation at 500 °C. Stiffness and ultimate bending strength of material 1, with low cobalt content, are only slightly affected by the temperature until 500 °C. By other side, material 2, with high cobalt content, shows a significant ductile deformation and also a significant decrease of ultimate bending strength and a slight increase of the fracture toughness with the temperature increasing until 500 °C. The brittle behaviour of the WC–Co alloys studied difficult fatigue pre-cracking of specimens for fracture toughness tests. An alternative approach based on unnotched specimens was used for material 2 with good results.

Fatigue S–N curve for material 1 were performed. No effect of the stress ratio was obtained at room temperature. This material exhibits slightly higher fatigue strength at 500 °C than at room temperature.

References

[1] Strenkowski JS, Carroll JT. A finite element model of orthogonal cutting. ASME J Eng Ind 1985;107:349–54.

[2] Cerreti E, Fallbohmer P, Wu W-T, Altan T. Application of 2D FEM to chip formation in orthogonal cutting. J Mater Process Technol 1996;59:169–81.

[3] Taylor FW. On the art of cutting metals. Trans Am Soc Mech Eng 1996;28:70–350.

[4] Shubert WD, Neumeister H, Kinger G, Lux B. Hardness to toughness relationship of fine-grained WC–Co hardmetals. Int J Refract Metals Hard Mater 1998;16:133–42.

[5] Ingelstrom N, Nordberg H. The fracture toughness of cemented tungsten carbides. Eng Fract Mech 1974;6:597–607.

[6] Ogilvy IM, Perrott CM, Suiter JW. On the indentation fracture of cemented carbide. Part 1-survey of operative fracture modes.. Wear 1977;43:239–52.

[7] Tanck E, Donkelaar CC, Jepsen KJ, Goldstein SA, Weinans H, Burger EH, et al. The mechanical consequences of mineralization in embryonic bone. Bone 2004;35:186–90.

[8] Antunes JM, Cavaleiro A, Menezes LF, Simões MI, Fernandes JV. Ultra-microhardness testing procedure with Vickers indenter. Surf Coatings Technol 2002;149:27–35.

[9] Rémond Y, Védrines M. Measurement of local elastic properties of injection moulded polymer structures by analysis of flexural resonant frequencies. Applications in POM, PA 66, filled PA 66.. Polym Test 2004;23:267–74.

[10] Taylor WR, Roland E, Ploeg H, Hertig D, Klabunde R, Warner MD, et al. Determination of orthotropic bone elastic constants using FEA and modal analysis. J Biomech 2002;35:767–73.

[11] Lauwagie T, Sol H, Heylen W, Roebben G. Determination of the in-plane elastic properties of the different layers of laminated plates by means of vibration testing and model updating. J Sound Vib 2004;274:529–46.

[12] Radovic M, Lara-Curzio E, Riester L. Comparison of different experimental techniques for determination of elastic properties of solids. Mater Sci Eng A 2004;368:56–70.

[13] Antunes FV, Ramalho A, Ferreira JAM, Capela C, Reis P. Determination of elastic properties by resonant technique: a sensitivity analysis. J Test Eval 2008;36:89–99.

[14] Jackson AP, Vincent JFV. Comparison of nacre with other ceramic composites. J Mater Sci 1990;25:3173–8.

[15] Hirsch TJ. Modulus of elasticity of concrete affected by elastic moduli of cement paste matrix and aggregate. J Am Concr Inst 1962;59:427–51.

[16] Llanes L, Torres Y, Anglada M. On the fatigue crack growth behavior of WC–Co cemented carbides: kinetics description, microstructural effects and fatigue sensitivity. Acta Mater 2002;50:2381–93.

[17] Torres Y, Casellas D, Anglada M, Llanes L. Fracture toughness evaluation of hardmetals: influence of testing procedure. Int J Refract Metals Hard Mater 2001;19:27–34.

[18] Kindermann P, Schlund P, Sockel H-G, Herr M, Heinrich W, Görting K, et al. High temperature fatigue of cemented carbides under cyclic loads. Int J Refract Metals Hard Mater 1999;17:55–68.

[19] Schijve J. Fatigue specimens for sheet and plate material. Fatigue Fract Eng Struct 1998;21:347–57.

[20] Ponton CB, Rawlings RD. Vickers indentation fracture toughness test. Part 1: review of literature and formulation of standardised toughness equations.. Mater Sci Technol 1989;5:865–72.

[21] Usami S, Kimono H, Takahashi I, Sida S. Strength of ceramic materials containing small flaws. Eng Fract Mech 1986;23:745–61.

[22] Torres Y, Anglada M, Llanes L. Evaluación de la tenacidade de fractura en carburos cementados tenaces, In: Proc XXI Encuentro del Grupo Español de Fractura, Punta Umbría. Anales de Mecánica de la Fractura 2004;21:338–43.

[23] Torres Y, Rodríguez S, Llanes L, Anglada M. Resistencia a la propagación de fisuras por fatiga en carburos cementados. Rev Metal 2001;37:145–9.

[24] Schleinkofer U, Sockel H-G, Gorting K, Heinrich W. Microstructural processes during subcritical crack growth in hard metals and cermets under cyclic loads. Mater Sci Eng A 1996;209:103–10.

[25] Schleinkofer U, Sockel H-G, Gorting K, Heinrich W. Fatigue of hard metals and cermets. Mater Sci Eng A 1996;209: 313–7.

[26] Roebuck B, Maderud CJ, Morrell R. Elevated temperature fatigue testing of hardmetals using notched testpieces. Int J Refract Metals Hard Mater 2008;26:19–27.